THE RADIOLOGICAL RESEARCH ACCELERATOR FACILITY

An NIH-Supported Resource Center

WWW.RARAF.ORG

Director: David J. Brenner, Ph.D., D.Sc.
Associate Director: Gerhard Randers-Pehrson, Ph.D.
Manager: Stephen A. Marino, M.S.

Research Using RARAF

The "bystander" effect - the response of cells that are not directly irradiated but are in close contact with, nearby, or only in the presence of irradiated cells - has been the focus for many of the biological studies at RARAF over the past two decades. Both the Microbeam and the Track Segment Facilities continue to be utilized in various investigations of this response to radiation exposure. This year the number of biological experiments investigating the mechanism(s) by which the effect is transmitted has declined somewhat, with newer

Table I. *Experiments Run at RARAF January 1 - December 31, 2013*

Exp No.	Experimenter	Institution	Exp. Type	Title of Experiment	Shifts Run
110	Tom K. Hei	CRR	Biol.	Identification of molecular signals of alpha particle-induced bystander mutagenesis	27.8
113	Alexandra Miller	AFRRI	Biol.	Role of alpha particle radiation in depleted uranium-induced cellular effects	1.9
147	Dalong Pang	Georgetown University	Phys.	LET dependence of DNA fragmentation by charged particles	0.8
152	Cary Zeitlin	Southwest Research Inst.	Phys.	Fast neutron detection efficiency of boron-loaded plastic scintillators	1.2
153	Howard Lieberman	CRR	Biol.	The role of Rad9 in mediating global gene expression in directly irradiated and bystander cells	2.9
157	Brian Ponnaiya	CRR	Biol.	γH2AX production by low-energy X-rays	1.2
160	Doug Spitz	University of Iowa	Biol.	Cellular oxidation of radiation-induced free radicals	1.5
163	Lubomir Smilenov	CRR	Biol.	Bystander effects in the hairless mouse ear	4.0
166	Andre Nussenzweig	NCI	Biol.	Chromatin restructuring as a function of microbeam-induced DNA DSBs	0.5
167	Eduoard Azzam	UMDNJ	Biol.	Radiation-induced DNA damage in bystander cells with inducible gap junction intercellular communication	3.0
168	Roger Howell	UMDNJ	Biol.	Bystander effects as a function of distance from irradiated cells in an *in vivo*-like system	1.9
169	Vincent LiCata	LSU	Biol.	The denatured states of a thermophilic versus a mesophilic DNA polymerase after charged particle irradiation	1.0
170	Ciaran Morrison	National Univ. of Ireland	Biol.	Live cell imaging of centrosome kinetics following microbeam irradiation	3.5
171	Peter Sims	Columbia University	Biol.	Single-molecule, single-gene expression following microbeam irradiation	0.1
172	Susan Bailey	Colorado State University	Biol.	Targeted telomeric damage and the persistent DNA damage response	3.0
173	Ekaterina Dadachova	Albert Einstein College of Medicine	Biol.	Comparison of fungal cell susceptibility to external alpha particle beam radiation versus alpha particles delivered by ^{213}Bi-labeled antibody	1.8

experiments starting to use the Microbeam Facility to examine damage to sub-nuclear structures (e.g., mitochondria, telomeres, and specific chromosomes) and other radiation effects. Research into bystander effects *in vivo* continued this past year with irradiations of the ears of mice.

Experiments

Listed in Table I are the experiments performed using the RARAF Singletron between January 1 and December 31, 2013 and the number of shifts each was run in this period. Fractional shifts are assigned when experimental time is shared among several users (e.g., track segment experiments) or when experiments run for significantly more or less than an 8-hour shift. Use of the accelerator for experiments was 23% of the regularly scheduled time (40 hours per week), about half of what was used last year but about the same as two years ago. Sixteen different experiments were run during this period. Four experiments were undertaken by members of the CRR, supported by grants from the National Institutes of Health (NIH), the National Cancer Institute (NCI), the National Institute of Allergies and Infectious Diseases (NIAID) and the National Institute of Biomedical Imaging and Bioengineering (NIBIB). Twelve experiments were performed by external users, supported by grants and awards from the Department of Energy (DoE), the Department of Defense (DoD), the NIH, the National Aeronautics and Space Administration (NASA), the National Science Foundation (NSF), the National Cancer Institute (NCI), the Economic Community Cooperation Programme, and internal funding from the Georgetown University Department of Radiation Medicine. Brief descriptions of these experiments follow.

A group led by Tom Hei of the CRR continued experiments investigating the effects of cytoplasmic irradiation and the radiation-induced bystander effect (Exp. 110). Using the Microbeam Facility, Jinhua Wu and Bo Zhang investigated mechanisms by which cytoplasmic stimuli modulate mitochondrial dynamics and functions in human small airway epithelial cells (SAECs). Their recent studies have shown that mitochondrial fragmentation induced by targeted cytoplasmic irradiation of human SAE cells is mediated by up-regulation of dynamin-regulated protein 1 (DRP1), a mitochondrial fission protein. To further explore the role of mitochondria in modulating the biological activities of high-LET radiation, autophagy in SAECs was examined. Autophagy was observed as early as 30 minutes after cytoplasmic irradiation with 10 alpha particles and peaked at 4 hours based on LC3B punctae formation. Sequestration of free radicals by DMSO abolished the induction of LC3B punctae formation, suggesting that activation of autophagy is free radical-dependent. Autophagy led to an increase of γ-H2AX foci that was dramatically reduced by choloroquine (CQ) or 3-methyladenine (3-MA), which are known inhibitors for autophagy. The DRP1 inhibitor mdivi-1 also significantly reduced autophagy, indicating that it plays a key role in activation of autophagy. DRP1 knockout HCT116 cells showed little or no autophagy after cytoplasmic irradiation, further confirming its role in autophagy induction. DRP1-dependent up-regulation of autophagy-initiating protein beclin-1 was also observed. Finally, a sustained activation of ERK was detected, suggesting potential involvement of the non-canonical MEK/ERK pathway in regulating autophagy in cytoplasmic irradiated cells.

Hongning Zhou irradiated mouse embryonic stem cells (mECSs) and mouse embryonic fibroblasts (MEFs) on double-ring "strip" dishes with ^{4}He ions using the Track Segment Facility. The outer ring has a 6 μm Mylar bottom through which the cells are irradiated by the ^{4}He ions while the inner dish has strips of 38 μm Mylar, which stop the ions. The results indicated that micronucleus formation was significantly induced in bystander and directly irradiated MEFs. However, only limited micronucleus formation was found in bystander mESCs, and even in mESCs directly irradiated with 0.5 Gy there was no significant increase in micronucleus induction compared to controls. In addition, 24 hours or 48 hours post irradiation a significant increase in dead (apoptotic and necrotic) cells was observed in both bystander and directly irradiated mESCs. Preliminary results from western blotting confirmed the findings, showing increased expression levels of cleaved caspase-3 and Poly (ADP-ribose) polymerase, an indicator of DNA damage. Furthermore, increased expression levels of β-catenin, NFκB, Smad2/3, p-Smad2/3, and cyclooxygenase-2 (COX-2) were observed in bystander and directly irradiated mESCs, which indicated that signaling through pathways such as TGFβ/Smad, NKκB, Wnt/β-catenin, and COX-2 pathways is involved in the regulation of the radiation-induced bystander effect in mESCs.

Alexandra Miller of the Armed Forces Radiobiological Research Institute (AFFRI) continued studies using the Track Segment Facility to evaluate depleted uranium (DU) radiation-induced carcinogenesis and other late effects using *in vitro* models and to test safe and efficacious medical countermeasures (Exp. 113). One objective of this study has been to determine if phenylbutyrate (PB), a histone deacetylase inhibitor and epigenetic effector, can mitigate neoplastic cell transformation induced by different qualities of radiation, and if so, to identify which adverse epigenetic mechanisms are involved and potentially reversed by PB. This also would be of interest for Space missions and alpha particle exposures from accidental releases. Track segment irradiations with ^{4}He ions were performed on human small airway epithelial cells (SAECs) and growth rate, transformation, and genomic instability were quantified. Irradiation of SAECs overcame contact inhibition and caused an increase in transformation frequency and induction of gene amplification, i.e., genomic instability. Treatment with PB following

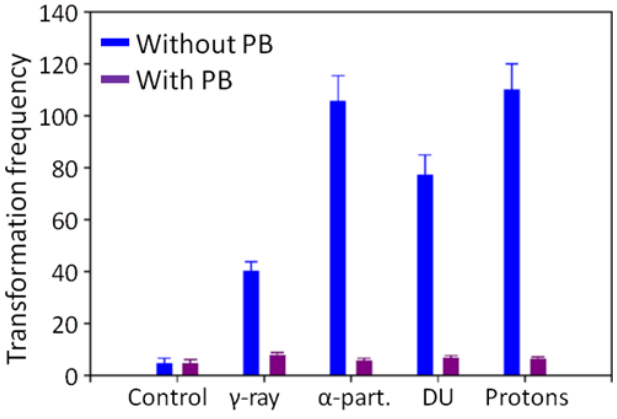

Figure 1. *Measured inhibition of neoplastic transformation by PB using RARAF alpha particles as compared to γ-rays, depleted uranium (DU), and protons.*

irradiation resulted in a significant suppression of transformation frequency (Figure 1) and gene amplification. Studies are ongoing evaluating the impact of PB treatment on changes in DNA methylation caused by irradiation with ^{4}He ions.

In a second part of the study, rodent bone marrow stromal cells were irradiated and co-cultured with unirradiated hematopoietic progenitor cells (FDC-P1). The FDC-P1 cells were monitored for the ability to grow in agar to assess neoplastic transformation. The data have demonstrated that co-culturing irradiated bone marrow stromal cells with FDC-P1 cells causes an increase in neoplastic transformation of FDC-P1 cells that involves the process of cell-cell communication. Additional mechanistic studies have shown that antioxidant processes are also involved in the non-targeted effect in FDC-P1 cells. Further studies with this model are ongoing evaluating involvement of non-targeted effects in multiple exposures at low doses (5 cGy).

A study of the LET dependence of DNA fragmentation was resumed by Dalong Pang of Georgetown University (Exp. 147) using the Track Segment Facility. Viral plasmids in solution were made into a thin layer of a known uniform thickness by pipetting a small volume onto a standard track segment dish, placing a cover slip on the liquid, and forcing the liquid to the edges of the cover slip. The DNA was irradiated with doses from 1 kGy to 8 kGy of 10 keV/µm protons. The irradiated DNA samples were subsequently analyzed using the atomic force microscope at Georgetown University. DNA fragment lengths were measured and grouped into various length intervals, and length-dose histograms were constructed. From the histograms, quantities such as the number of double-strand breaks (DSB) per DNA and the spatial distribution of DSB on a DNA molecule were derived.

Cary Zeitlin of the Southwest Research Institute, along with several colleagues, continued to characterize the efficiency of a neutron spectrometer based on a boron-loaded plastic scintillator (Exp. 153) for use in Space. Neutrons are thermalized in the large detector as they lose energy in elastic collisions, primarily with the hydrogen nuclei in the scintillator material. Since these collisions occur extremely rapidly, the energy deposited by the neutron can be observed as a single pulse. The low-energy neutrons are often captured by the boron, which has a very large thermal neutron cross section and releases a 1.5 MeV alpha particle a very short time after the pulse from the neutron collisions. The pulse from this alpha particle is of constant amplitude and indicates that the initial pulse was caused by a neutron that has given up all its energy in the detector. An advantage of this design is the direct measurement of the neutron energy spectrum. Most other spectroscopy systems require complicated deconvolution programs. The detector was irradiated with essentially monoenergetic neutrons in the range from 0.5 to 2.5 MeV to determine detector efficiency.

Howard Lieberman, Sally Amundson, Shanaz Ghandhi, Sunil Panigrahi, and Kevin Hopkins continued investigations of the effects of Rad9 on radiation-induced changes in gene expression in human cells directly irradiated or as bystanders (Exp. 153). Using shRNA against RAD9, the expression of RAD9 was knocked down in the human prostate cancer cell line DU145. The RAD9 knocked-down DU145 cells were seeded onto double-ring "strip" dishes (described above) and irradiated with ^{4}He ions using the Track Segment Facility. Both irradiated and bystander cells were of the same type and the signaling was through cell-to-cell contact and also through factors released into the medium. Additional irradiations were made using spacer dishes in which cells are plated on Mylar glued to a stainless steel ring and the ring is inserted into a standard track segment dish so that the cells on the ring are not in direct contact with the cells irradiated on the dish. In these experiments, the DU145 cells were irradiated, WPMY1 or prSMC cells were the bystander cells, and signaling is only possible through molecules secreted by the irradiated cells. After irradiation, bystander response was measured by the micronucleus assay. An increase in micronucleus count was observed in the RAD9 knockdown cells as compared to the parental cells, which suggests RAD9 plays a role in the radiation-induced bystander effect. Future studies will investigate the mechanisms involved in this process.

Brian Ponnaiya of the CRR performed additional irradiations for a study of the production of γH2AX foci by low-energy x rays using the X-ray Microbeam Facility (Exp. 157). Cells were irradiated in media with 0.1 and 0.2 Gy of 4.5 keV x rays. The γH2AX foci were detected using anti human γH2AX monoclonal antibody, visualized using an Alexa Fluor 555 secondary antibody, and the nuclei were counterstained with DAPI. Fluorescent images were acquired and mean fluorescence intensities of a minimum of 150 individual cells were measured.

Doug Spitz of the University of Iowa, in collaboration with Manuela Buonanno, continued an investigation

designed to evaluate whether cells respond with different ROS signals following nuclear versus cytoplasmic irradiation (Exp. 160). Mouse embryo fibroblasts (MEFs) were irradiated with 1 or 10 ^{4}He ions (90 keV/μm) using the Microbeam Facility. It was observed using MitoSOX and DHE dyes that both nuclear and cytoplasmic irradiations resulted in elevated nuclear fluorescence as early as 5 min post-irradiation, presumably indicating elevated levels of superoxides. The elevated nuclear signals were observed up to 24 hours later. Significantly, treatment with 150 nM DPI, a known inhibitor of nuclear oxidases, attenuated these responses. Since MitoSOX and DHE are not specific, in that the fluorescence could be due to intracellular or mitochondrial superoxides, and the emission spectra of the two fluorescent species are overlapping and difficult to separate by standard fluorescence microscopy, further investigations will need to be performed. The two dyes will be separated by capillary electrophoresis and observed by laser induced fluorescence detection (CE-LIF).

Lubomir Smilenov and Manuela Buonanno of the CRR are examining the bystander effect *in vivo*, irradiating mouse ears using the Microbeam Facility (Exp. 163). A special fixture has been designed and constructed in the CRR machine shop to position anesthetized mice so that a region on one ear can be irradiated with the microbeam, the other ear serving as a control. The mouse ear has an average thickness of 250 μm. A 3 MeV proton beam with a range of ~134 μm was defocused to a diameter of ~35 μm and scanned in a line a few mm long in order to irradiate a larger number of cells. At chosen times after irradiation, mice were sacrificed and a punch of the ear was collected. Tissues were then fixed, paraffin-embedded and cut in 5-μm sections perpendicular to the direction of the charged particle beam. As expected, cells in the epidermal layer opposite to the γH2AX-positive region, well beyond where the beam penetrated, did not exhibit foci. The average width spanned by γH2AX-positive cells exceeded 150 μm, however, significantly larger than the proton beam width. These results suggest that microbeam proton irradiation induced DNA damage in bystander cells *in vivo*. Ongoing experiments aim at investigating the kinetics of DNA repair foci formation and apoptosis in microbeam-irradiated ears. Further, the biological effects of smaller-diameter proton microbeams will be investigated.

A study by Andre Nussenzweig of the NCI, in collaboration with Brian Ponnaiya, of the mobility and restructuring of chromatin as a function of induced DNA double strand breaks (DSBs) using the Microbeam Facility (Exp. 166) continued this year. The UV microspot was used to photoactivate a single spot in Hela cells containing a photoactivatable version of GFP-tagged histone H2B (H2B-PAGFP). This spot was imaged using a 60X 1.0 NA immersion objective and irradiated with 25 or 50 ^{4}He ions. Cells were imaged every 5 min for up to 1 hour in multiple planes through the cell and the image stacks were sent to the PI for subsequent analyses. Tests are ongoing to determine the minimum laser power required to activate a sufficient amount of GFP in as small an area as possible and the time course required for observations.

Eduoard Azzam of Rutgers University (formerly the University of Medicine and Dentistry of New Jersey), in collaboration with Manuela Buonanno, continued a study of radiation-induced DNA damage in bystander cells using cells with inducible gap junction intercellular communication (Exp. 167). The nuclei of ten percent of HeLa cells with chemically inducible Connexin-26 (Cx26) were irradiated with one ^{4}He ion using the Microbeam Facility. Compared to controls, cultures both positive and negative for Cx26 exhibited a statistically significant increase of cells with γH2AX foci, however, chemical induction of Cx26 reduced the level of foci.

An investigation of bystander effects in an *in vivo*-like system as a function of the distance from irradiated cells (Exp. 168) was continued by Roger Howell of Rutgers University in collaboration with Manuela Buonanno. Normal human fibroblasts (AG1522) mixed in a biogel (Matrigel) were loaded onto 3D carbon foam scaffolds (cytomatrices) 8.75 mm in diameter and 2 mm thick and irradiated with He ions using the Track Segment Facility. The ions have a range of ~35 μm in the cytomatrix, so that only the first few cell layers are irradiated; the cells beyond the particle range are bystanders. In situ assays were performed to investigate DNA damage, cell death and micronucleus formation. The best results were observed with radiation-induced 53BP1 foci formation. Cells with foci could be detected up to 60 μm away from the irradiated cell layers.

Vincent LiCata of Louisiana State University continued an investigation of whether proteins from radiation resistant organisms are radiation resistant when isolated from the organism (Exp. 169). Homologous DNA binding proteins from organisms that live under very different conditions were examined, one of which was the extremely radiation-resistant bacterium Deinococcus radiodurans. As for Experiment 147, protein in solution was formed into a layer with a known uniform thickness under a cover slide. In order to obtain sufficient material, multiple samples were given doses of 5 to 20 kGy of 4.0 MeV protons at dose rates in excess of 1 kGy/min using the Track Segment Facility. Protein stability and function were assayed to determine whether the DNA polymerase from D. radiodurans is better able to withstand radiation exposure than are homologous proteins from non-radiation-resistant organisms. The primary focus is on so-called secondary radiation effects, such as damage by reactive oxygen species, rather than direct hit effects, as the secondary effects are responsible for the majority of damage in biological systems.

Ciaran Morrison of the National University of Ireland, in collaboration with Brian Ponnaiya, initiated a study probing the mechanisms involved in the process of

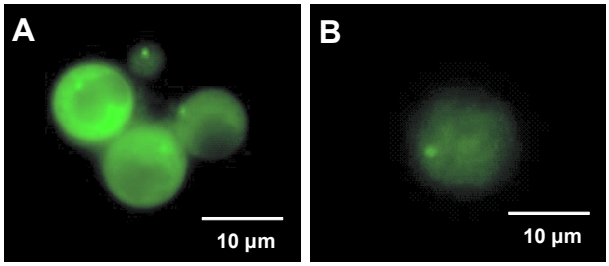

Figure 2: *DT40 cells expressing centrosome-associated proteins Chibby-GFP (A) and Centrin3-GFP (B) grown on poly L-lysine on microbeam dishes.*

unscheduled centrosome duplication as a consequence of exposure to ionizing radiation at defined nuclear sites using the Microbeam Facility (Exp. 170). Initial experiments using DT40 chicken lymphocytes were conducted to a) test the ability of the cells to adhere to a substrate, and b) assess the viability of these cells over the time span proposed for the experiments (48 h). Cells were seeded onto poly L-lysine-coated 60 mm dishes and imaged (Figure 2) for irradiation on the microbeam endstation.

A microfluidic platform to study individual mRNA molecules in single cells is being developed by Peter Sims, of the Joint Center for Systems Biology of Columbia University. In his device, single cells are deposited in microwells and lysed in situ. The mRNA contents are then captured in the well and individual mRNA molecules are counted following reverse transcription and fluorescence detection by hybridization to transcript-specific cDNA probes labeled with Sytox Orange. The response of his device is being tested in collaboration with Brian Ponnaiya by examining the radiation-induced gene expression changes in individual cells (Exp. 171). Experiments conducted using the Microbeam Facility have demonstrated detection of single molecules of GAPDH in cells grown on microbeam dishes and irradiated with ^{4}He ions. Experiments to examine radiation responsive genes, i.e., CDKN1A and GADD45A, following microbeam irradiation are continuing.

Susan Bailey at Colorado State University, in collaboration with Brian Ponnaiya, is using the Microbeam Facility to target telomeres and examine the repair processes at these chromosome ends (Exp. 172). Preliminary studies were conducted to develop a cell system to perform these experiments. As a first step, fluorescent 53BP1 and TRF1 constructs were coexpressed in HT1080 cells and imaged at the microbeam endstation (Figure 3). The fluorescent spots of TRF1-GFP serve as microbeam targets and the cells will be followed in time to examine the co-localization of 53BP1 to the irradiated sites.

Ekaterina Dadachova at the Albert Einstein College of Medicine has been developing radioimmunotherapy (RIT) for treatment of Cryptococcus neoformans infections using ^{213}Bi-labeled antibodies specific to the cryptococcal

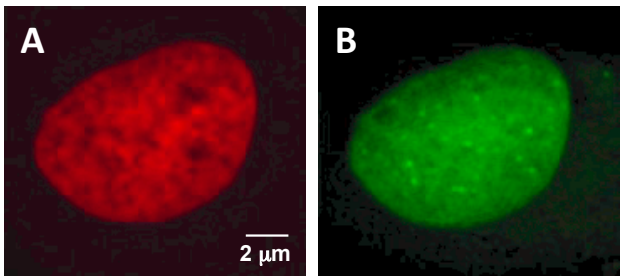

Figure 3: *Coexpression of the DNA repair protein 53BP1-mCherry (A) and TRF1-GFP (B) stably transfected in HT1080 cells. (TRF1 vector courtesy of Dr. Elizabeth Blackburn).*

capsule. She is performing a comparison of fungal cell susceptibility to external α-particle beam radiation versus α particles delivered by the bismuth-labeled antibodies (Exp. 173). Fungi grown to stationary phase in defined minimal medium were suspended in solution. As for other experiments, the solution was formed into a thin layer with a known uniform thickness under a cover slip. The fungi were irradiated with doses of 1 to 80 Gy of 125 keV/µm ^{4}He ions. Results so far indicate that: a) C. neoformans is more sensitive to external beam α particles than to external γ rays; b) α particles delivered by the capsule-binding antibodies may be more cytocidal to the C. neoformans cells than external beam α particles.

In addition to these experiments that use ionizing radiation, the ultraviolet (UV) microspot is being used by Kimara Targoff in the Division of Pediatric Medicine of Columbia University as an irradiation modality to observe the consequences of the ablation of single cells in the development of the embryonic zebrafish heart (Exp. 162). Unlike the charged particle microbeams, the UV microspot only produces damage in the focal spot (approximately 1 µm diameter, 1.5 µm long), thus producing minimal effect elsewhere along the beam path. Cardiomyocytes in the ventricles of the hearts of zebrafish embryos are transfected with red fluorescent protein (RFP). The exposure protocol involves imaging cells on the top ventricular surface of the heart, where the incident laser first transits the ventricle, in live embryos 52 hours post fertilization and identifying individual cell nuclei as targets. Each cellular target exposure is a sequence of three co-planar UV microspot scans over a 17.5 x 17.5 µm^2 area about each cell nucleus. The incident laser wavelength is tuned to 700 nm (350 nm during two-photon absorption) and the total exposure energy per cell is 27 mJ, corresponding to 18 mW exposure power during the 1.5 s exposure time. Consequences of UV microspot damage are monitored by live imaging, in situ hybridization, and immunostaining.

Development of Facilities

Development continued on a number of extensions of our irradiation facilities and capabilities for imaging and irradiating biological specimens:

- Focused particle microbeams
- Focused x-ray microbeam

- Neutron microbeam
- Hiroshima bomb spectrum neutron source
- Advanced imaging systems
- Targeting and manipulation of cells
- New cell analysis tools
- Small animal systems

Focused particle microbeams

The electrostatically focused microbeam has continued to operate very reliably this past year, consistently producing a beam spot 1-2 μm in diameter using the standard 500 nm thick silicon nitride exit window. When a sub-micron beam spot is desired, a window only 100 nm thick, which has a much smaller area and is more fragile, is used.

For quality control we perform a microbeam test run the evening before an irradiation so that the next morning, after the accelerator has warmed up, the charged particle beam is found immediately and has a minimal beam spot diameter. This provides an earlier and trouble-free start for irradiations and consequently a greater throughput.

A new, "super-microbeam" is being designed to focus a charged particle beam of protons up to 3 MeV and ^{4}He ions up to 6 MeV to a focal spot <100 nm in diameter. The system will consist of a superconducting magnetic solenoid lens and either an electrostatic quadrupole quadruplet or the pair of quadrupole triplets presently used to focus the beam. The design should be finalized by mid-2014.

The permanent magnet microbeam (PMM) uses a compound quadrupole triplet lens system made from commercially available precision permanent magnets. Its design is similar to that of the electrostatic lens system for the sub-micron microbeam, the major difference being that it uses magnetic rather than electrostatic lenses. The quadrupole magnet strengths used to focus the beam have been adjusted to produce a focused 4.4 MeV proton beam for development of the Flow and ShooT (FAST) microfluidics system (described below).

Focused x-ray microbeam

The x-ray microbeam provides characteristic Kα x rays generated by proton-induced x-ray emission (PIXE) from Ti (4.5 keV). A small x-ray source is produced by bombarding a Ti target with 1.8 MeV protons using a single electrostatic quadrupole quadruplet lens to focus the beam to ~50 x 120 μm^2 on the target. Charged particle beams can generate nearly monochromatic x rays because, unlike electrons, protons have a very low bremsstrahlung yield.

X rays emitted at 90° to the proton beam direction are focused to a beam spot 5 μm in diameter using a zone plate 120 μm in diameter. The system is mounted on its own horizontal beam line on the first floor of RARAF and the x-ray beam is oriented vertically, so that the geometry of the microscope and stage is the same as for our charged particle microbeam systems.

Neutron microbeam

The first neutron microbeam in the world has been developed at RARAF.

When the proton energy is just above the reaction threshold of the ^{7}Li(p,n)^{7}Be reaction (1.881 MeV), neutrons are emitted only in a forward conical volume. The half-angle of this cone is dependent on the proton energy and increases with increasing energy. A focused proton microbeam 10 μm in diameter is incident on a 1-μm thick lithium fluoride target deposited on a 25-μm thick gold backing (selected for its high density and thermal conductivity), which stops the incident protons. Using a 1.886 MeV proton beam, cells on a thin polypropylene substrate that is in contact with the target backing are exposed to a beam of neutrons having energies from 10-50 keV that is geometrically restricted to a diameter of 36 μm at the location of the cells. A beam current of 10 nA has been achieved, yielding a dose rate of ~27 mGy/min.

The facility has been constructed on a dedicated horizontal beamline using a single quadrupole quadruplet to focus the proton beam. In order to measure the proton beam spot size, a thin Havar metal window is used in place of the gold target. The protons pass through this window and the beam spot size is determined in the same manner as for the PMM proton microbeam: a knife-edge scan using 10 μm thick tantalum strips in order to reduce the proton energy significantly. Unlike the other microbeams, in which the charged particle or x-ray fluence is relatively low, the proton beam current for the neutron microbeam is of the order of 1 nA (6×10^9 protons/s) – too high to count, so an ionization chamber, instead of a solid state detector, is used to observe the change in the proton beam as it is scanned. The location of the center of the proton beam, which is also the location of the center of the neutron microbeam, can be optically observed by using a very thin scintillator.

The size of the neutron beam was measured using CR-39 track-etch plastic. Because the recoil protons generated by the neutrons do not make observable pits, the CR-39 is coated with a thin layer of lithium carbonate heavily enriched in ^{6}Li. The neutrons interact with the ^{6}Li through the ^{6}Li(p,α)^{3}H reaction, producing energetic α and ^{3}H recoils that are easily observable as pits in the etched CR-39 using a microscope.

Hiroshima bomb spectrum neutron source

Development has continued on a fast neutron source with a broad spectrum that will emulate that of the "Little Boy" atomic bomb at Hiroshima. A mixed beam of 5 MeV monatomic, diatomic and triatomic protons and deuterons incident on a thick beryllium target produces neutrons from the ^{9}Be(d,n)^{10}B and ^{9}Be(p,n)^{9}B reactions. The diatomic and triatomic particles break up on contact with the target into individual ions with 2.5 MeV and 1.67 MeV energies, respectively, enhancing the lower-energy portion of the spectrum. In order to produce this mixed ion beam, a gas source with a ratio of hydrogen to

deuterium of 1:2 has been placed in the terminal of our Singletron accelerator and a new, 0º beam line has been installed. Since this beam line does not involve deflecting the particle beam from the accelerator, there is no separation of the different ions and the full beam from the accelerator is utilized.

To determine the energy spectrum of this broad-energy neutron facility, a 2 inch diameter by 2 inch high detector filled with EJ-301 liquid scintillator was chosen for the energy range >1 MeV. This liquid scintillator has good rise time characteristics for neutron-gamma discrimination, however there is a low-energy cutoff because its efficiency declines with neutron energy and there is a cut-off due to the gamma-ray discrimination. A 1.5-inch diameter spherical gas proportional counter filled with 3 atmospheres of hydrogen gas will be used to measure the spectrum below 1 MeV. This detector has an upper energy limit because many high-energy recoil proton tracks are truncated at the wall of the detector. Eight monoenergetic neutron spectra with energies between 0.5 and 8 MeV have been measured with the scintillation detector and unfolded using response functions calculated using the MCNPX-PoliMi Monte Carlo program.

Preliminary dosimetry indicates a total dose rate at the position of the samples to be irradiated of ~0.13 Gy/hr/μA of beam with a gamma-ray contribution of ~15%. This easily will provide a sufficient dose rate to give samples 1 Gy of neutrons in less than 1 hour.

The area in which the new 0º beamline has been constructed has much less shielding than the neutron cave that has traditionally been used for irradiations. Because of the high neutron dose rate that is produced, as well as the high energy of some of the neutrons, additional shielding has been added above the target position and in the maze entrance to the area. A radiation survey has been performed using the 5 MeV mixed proton/deuteron beam. Although the dose rate outside the radiation area was greatly reduced, additional shielding will be added and another survey made.

Advanced imaging systems

We continue to develop new techniques to obtain two- and three-dimensional images of cells, reduce UV exposure and improve resolution.

Real-time imaging

Techniques have been developed using our EMCCD camera and our fast switching SOLA LED light source to acquire images with several frames per second to observe the short-term effects of irradiation on a timescale of minutes to hours following irradiation. Short-term effects that happen within seconds to the first few minutes after irradiation set the stage for later effects. Real-time imaging and observation of the short-term effects will give insight to experimenters into their end points.

UV microspot

A multi-photon microscope was developed and integrated into the microscope of the Microbeam Facility several years ago to detect and observe the short-term molecular kinetics of radiation response in living cells and to permit imaging in thick targets, such as tissue samples and C. elegans. Two photons delivered very closely together in space and time can act as a single photon with half the wavelength (twice the energy). The longer wavelength of the incident light beam allows better penetration into the sample and excitation of fluorophors at the focal volume while producing less damage in the portion of the sample not in the focal volume. By using the vertical motion of the microbeam stage, a series of images acquired at different depths in the sample can be assembled into a 3-D image.

Several users, both internal and external, have made use of this facility this year for 3-D imaging. This system is also being used as a laser "microspot" to induce UV damage in the cells in the ventricle of zebrafish embryos (Targoff, Exp. 162).

STED

As we design a new microbeam system capable of focusing a charged particle beam to <100 nm, the resolution of our imaging systems must be improved to resolve ever-smaller targets. Our present imaging system is limited by diffraction to a resolution of ~200 nm. Stimulated Emission Depletion (STED) has been selected as a super-resolution system for the new microbeam since it is compatible with our aim for rapid imaging and can be developed using our existing multiphoton microscope system as the excitation laser.

Stimulated emission happens at a specific longer wavelength than the typical relaxation/emission wavelength. By using a laser with longer wavelength (STED laser) than the imaging fluorophor to produce a ring of stimulated emission, it is possible to deplete the excited fluorophors around the edge of an excitation spot creating a sub-100 nm diameter area where fluorescence is still possible. This concept is being extended to live-cell imaging in medium.

Tests of imaging live cells using an immersion objective have been made with the custom STED system developed by our consultant, Dr. Liao from the Mechanical Engineering Department at Columbia University. Although this system was not optimized for imaging through media, it was possible to locate single mitochondria in live cells with sub-100 nm resolution. Our STED system will be based on the design used by Dr. Liao and requires the acquisition and installation of a high-power continuous wave (CW) STED laser.

Targeting and manipulation of cells

We have the capability to fabricate microfluidic devices in hard plastics, such as acrylic, and soft plastics, such as polydimethylsiloxane (PDMS). Several of our staff now have experience with the micro-milling

machine installed at RARAF and have familiarized themselves with the software that programs the milling machine to produce parts designed using the Solid Works computer-aided design (CAD) program. This system has been used to manufacture the single-cell dispenser and the microfluidics chips for the cell sorter and microFACS systems (described below). It has greatly reduced the need to use Mechanical Engineering Department facilities at the Morningside campus of Columbia, saving time and increasing convenience. Several new microfluidic systems are being developed to target, manipulate and analyze cells.

FAST

Development has essentially been completed on the microfluidic Flow And ShooT (FAST) targeting system that increases the throughput of the PMM and provides irradiation of non-adherent cells, such as lymphocytes, that do not plate on surfaces and therefore do not have stable positions.

Cells moving through a narrow channel are imaged by a high-speed camera (tens to hundreds of frames/s) to track their trajectory. The Point and Shoot magnetic deflection system is used to aim the particle beam to the projected position of the cell on the trajectory and the particle beam is enabled. The deflection coil currents are changed continuously to follow the path of the cell until the required number of particles is delivered. The system is capable of tracking several cells at a time.

We manufacture the required PDMS microfluidic chips ourselves using soft lithography. The channel is 200 µm wide and 20 µm high, so that the cells, when targeted by the microbeam, flow in the immediate vicinity of the microbeam exit window. The bottom of the irradiation section of the microfluidic channel is 10 µm thick and the top is 20 µm thick, so particles can reach the cells and the detector above the channel. The flow rate is controlled by a syringe pump.

Implementation of high numerical aperture optics into the imaging system and improvement in image processing speed has resulted in the ability to target cells moving at a speed of ~500 µm/s, with a throughput of 10,000 cells / h. At present, the targeted position agrees with the true position within ±1.5 µm more than 95% of the time.

Cell dispenser

Another cell manipulation device that is under development is a single-cell dispenser, which consists of a microfluidic channel in which selected cells can be dispensed into a multi-well plate. In a system where cells normally travel across a T-intersection, a pressure pulse can eject a droplet containing a single cell into the channel normal to the flow as it passes the nozzle. The device is made from a polymethyl methacrylate (PMMA) slab with 100 µm x 50 µm channels directly milled using the micro-milling machine at RARAF.

This system is presently manual, very laborious, and very inefficient, requiring the operator to observe cell fluorescence through a microscope and activate a switch to select the desired cells. Cell flow rate has to be kept low to accommodate operator reaction time.

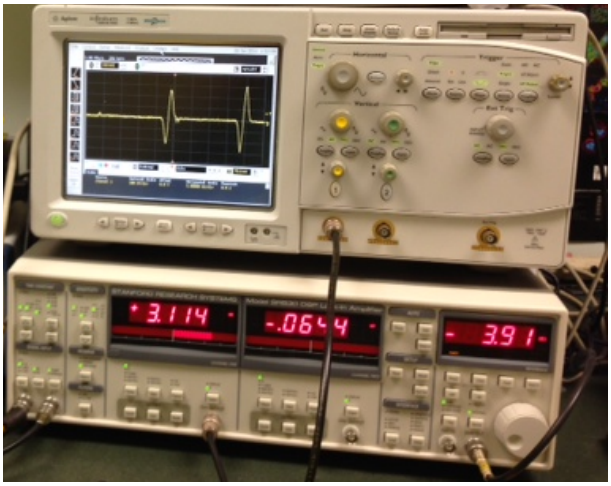

Figure 4. *The SR830 lock-in amplifier (bottom) output is shown on an oscilloscope (top). Each pulse indicates a transient change in impedance caused by a cell passing microelectrodes within a microfluidic channel.*

Automation of the cell dispensing system is underway. Cells suspended in a solution alter the resistive and capacitive properties of the solution. These impedance changes can be detected using microelectrodes integrated in the microfluidic chip. An SR830 lock-in amplifier (Figure 4) is used to detect differential impedance changes in a bridge circuit configuration where two opposing impedance arms of the circuit are measured through the cell solution using the microelectrodes. The lock-in amplifier measures the AC impedance, which includes both the resistive and capacitive components. The use of AC impedance prevents microelectrode polarization, which would alter DC resistance measurements, as well as causing bubble formation through hydrolysis. Using this system we have detected individual cells passing through a microfluidic channel (Figure 4).

MicroFACS

A microfluidic Fluorescence-Activated Cell Sorting (microFACS) system is being developed that combines flow cytometry and cell sorting into one microfluidic device. This will provide the capability of flow sorting for irradiation, particularly in tandem with our other microfluidic systems.

The microFACS system uses Dean vortex flow focusing to focus the flow of a cell into the center of a microfluidic channel. This column is illuminated with lasers brought into the system through fiber optic cables. The scattered incident light and fluorescent signals from the cells are collected through additional fiber optics without the use of lenses. Based on these signals, the cells are scored and sorted immediately downstream from the inspection point using the automated microfluidic cell

sorter. Detection of single-cells has been demonstrated in our micro-machined, hard plastic (polycarbonate) system.

AMOEBA

Automated platforms integrated with our microbeam systems are being developed to provide precise regulation and control of environmental conditions for biological samples before, during and at long times after microbeam irradiation. These systems will allow for establishing, maintaining and changing conditions (e.g., temperature, pH, pCO_2, pO_2, and drug concentrations) for the culture environments surrounding cells, tissues, and small organisms to enable short- and long-term observations in situ within the microbeam irradiation platforms. Two different, though similarly motivated systems are being developed: AMOEBA (Automated Microbeam Observation Environment for Biological Analyses) and μAMOEBA, a microfluidics version. Both will be automated, feedback-based, fluid-flow systems using essentially the same control electronics.

The AMOEBA system is compatible with standard dish-based microbeam experiments and is designed to facilitate tight environmental controls over long periods; μAMOEBA allows precise microfluidics-based control and rapid changes of environmental parameters, such as hypoxia, and also the use of much smaller volumes of material. These developments will support extended-time experiments, such as those involving monitoring the kinetics of DNA repair, cell-cycle progression, and chromosomal domain dynamics. To establish proper pH control outside an incubator, we have included in our AMOEBA design a mechanism to regulate the CO_2 gas mixture flow over the medium and thus control media pH. We also have established constant temperature control in a prototype AMOEBA system that can maintain system temperature at 37 ± 1 °C over extended periods without using feedback control.

New cell analysis tools

CE-LIF

In order to provide our users with the capability to measure reactive species within individual cells after inducing single-cell or sub-cellular damage, we have begun designing and testing a Capillary Electrophoresis - Laser Induced Fluorescence (CE-LIF) system coupled to our microbeam. The nanoliter sample sizes used in CE make this technique suitable for small-scale biochemical applications and, in particular, for single-cell studies.

The basic idea of CE is to take advantage of two superimposed flow modalities experienced by the analytes in a long, thin fused silica capillary: (1) Electrophoretic flow, responsible for separating the analytes of lysed cells by charge and Stokes radius; (2) Electroosmotic flow, which drives the buffer and analytes (regardless of polarity) toward the detector. The electroosmotic flow is much stronger than the electrophoretic flow, ensuring that all analytes will reach the detector. Coupled to CE, laser-induced fluorescence (LIF) provides highly sensitive detection, particularly for brightly fluorescent molecules.

A series of studies, performed at RARAF and in the lab of Dr. Jonathan Sweedler at the University of Illinois (Urbana-Champaign), have demonstrated that single-cell CE-LIF does have sufficient sensitivity to investigate various radiation-relevant endpoints (e.g., glutathione levels and oxidation of redox-sensitive dyes, such as DHR-123). These studies have provided us with the preliminary data required to build a CE-LIF system at RARAF and directly couple it to the Microbeam Facility.

Single-cell Raman spectroscopy

Plans have been established for a unique coupling of our microbeam irradiator with a commercial Raman spectroscopy system to provide a technique for non-invasive, label-free identification and assessment of the distribution of bio-molecules and chemicals within single cells in real time. In the context of radiation-induced biological damage, Raman spectroscopy effectively probes conformational changes in large biomolecules / chromatin and there is rapidly increasing interest in this technique for single-cell analysis. This innovative coupling of technologies at RARAF will produce the first microbeam facility with on-line Raman spectroscopy capacity for studying radiation response in single cells and single cells within 3-D tissues, where the same cell can be sampled before irradiation and at times post-irradiation.

Extensive experience in single-cell Raman spectroscopy has been acquired using a Renishaw inVia Raman spectrometer located in the Electrical Engineering Department at Columbia University, the same model as proposed in the RARAF system. An important aspect of the study was that immersion optics were used during the Raman analysis. In addition to allowing for broad-field visualization of single cells in a tissue slice, this technique significantly enhanced the Raman signal intensities that were obtained, allowing for decreased acquisition times. This system has been used successfully to measure single-cell Raman spectra in a 3D full-thickness model of human skin (MatTek Corp.).

Small animal systems – Transgenic mouse model

Investigations of radiation-induced bystander effects have been conducted in cell cultures and 3-D systems *in vitro*. The next logical step was to develop and implement microbeam irradiation protocols to study effects in living organisms. We have developed a mouse ear model for *in vivo* bystander studies. With an average thickness of 250-300 μm, this model can be used to investigate radiation-induced bystander effects with a 3-MeV proton microbeam having a range of 134 μm.

Using gentle suction, the ear of an anesthetized mouse is flattened onto the underside of a flat plate of a custom-made holder. The flattened mouse ear is then placed over the microbeam port and cells along a line of the ear are irradiated with the proton microbeam. At chosen times

after irradiation, mice are sacrificed and a punch of the ear is collected. Tissues are then fixed, paraffin-embedded and cut in 5-μm sections perpendicularly to the direction of the line of irradiation. The sections are then analyzed for biological endpoints (i.e., formation of repair protein foci, apoptosis) as a function of the distance from the irradiated line.

Using γH2AX foci formation assessed by immunohistochemical analysis as an endpoint, we found that proton irradiation induced γH2AX foci formation *in vivo* relative to controls. As expected, γH2AX foci-positive keratinocytes were observed in only one of the two epidermal layers of the mouse ear. Cells in the epidermal layer opposite to the irradiated γH2AX positive region did not exhibit foci. Assuming that the nuclei of mouse keratinocytes are 9-11 μm in diameter, a larger number of cells than expected showed foci. In a particular experiment, although the irradiated line was ~35 μm wide, the average width spanned by γH2AX-positive cells exceeded 150 μm. These results suggest that microbeam proton irradiation induced DNA damage in bystander cells *in vivo*.

Singletron Utilization and Operation

Table II summarizes accelerator usage for the past year. The nominal Singletron availability is one 8-hour shift per weekday (~248 shifts per year), however the accelerator is frequently run well into the evening, often on weekends, and occasionally 24 hours a day for experiments or development. Total use for experiments and development this year was 50% of the regularly scheduled time.

Accelerator use for radiobiology and associated dosimetry was about half that for last year and about 2/3 the average for the last 5 years. About 70% of the use for all experiments was for charged particle microbeam irradiations, 27% for track segment irradiations, and 2% for neutron irradiations. Approximately 40% of the experiment time was for studies proposed by external users, and 60% was for internal users.

Table II. *Accelerator Use, January 1 - December 31, 2013*
Normally Scheduled Shifts

Radiobiology and associated dosimetry	22%
Radiological physics and chemistry	1%
On-line facility development and testing	27%
Microbeam Training Course	1%
Safety system	1%
Accelerator-related repairs/maintenance	5%
Other repairs and maintenance	1%
Off-line facility development	60%

On-line facility development and testing was about 27% of the available time, primarily for development and testing of the neutron microbeam and the Hiroshima neutron spectrum system and for testing the charged particle microbeam prior to scheduled irradiations. This was about 20% less than the average for the last five years and about half as much as last year due to a much larger emphasis on development not requiring accelerator use.

The accelerator was opened twice this year: once to replace the ion source after two years of use, the second time to install in the terminal a gas cylinder containing a hydrogen-deuterium gas mixture to produce the ion beam for the Hiroshima bomb spectrum facility. During the second opening, problems were observed with a couple of the bearings on the shaft in the Singletron that drives the generator to provide power in the terminal and they were replaced. This was the first repair to the accelerator due to wear (other than for the ion source) in the ~10,000 hours of operation since it was installed in December, 2005.

Training

REU

Since 2004 we have participated in the Research Experiences for Undergraduates (REU) project in collaboration with the Columbia University Physics Department. This is a very selective program that attracts highly talented participants. For 9-10 weeks during the summer each student attends lectures by members of different research groups at Nevis Laboratories, works on a research project, and presents oral and written reports on his or her progress at the end of the program. Among other activities, the students receive a seminar about and take a tour of RARAF.

This year Tabatha Felter from Cornell University participated in the program and worked with Yanping Xu on the development of an unfolding code for determining the neutron spectrum of the Hiroshima bomb neutron spectrum irradiation facility from the measured proton recoil spectra.

Microbeam Training Course

The third annual RARAF microbeam training course "Single-Cell Microbeams: Theory and Practice" was given May 20-22, 2013. There were again eight students, which is about the largest number we can reasonably handle.

Dr. Marcelo Vazquez of Loma Linda University Medical Center continued his service as Course Director. He has had significant experience from his prior employment at the NASA Space Radiation Laboratory (NSRL) at Brookhaven National Laboratory (BNL) where he helped establish the first NASA Space Radiation Summer School and ran the course for three years.

Table III. *Students for the third RARAF Microbeam Training Course.*

Name	*Position*	*Affiliation*
Po Bian	Research Scientist	Key Lab of Ion Beam Bioengineering, Chinese Academy of Sciences
Liang Chen	Postdoctoral Res. Fellow	Earth Science Division, LBNL
Jason Domogauer	MD/Ph. D. student	University of Medicine and Dentistry of NJ
Geraldine Gonom	Postdoctoral Res. Scientist	Institut de Radioprotection et de Sûreté Nucléaire, France
Jian Gu	Assistant Professor	The Univ. of Arizona College of Medicine
Wayne Nicholson	Professor	University of Florida, NASA
Erik Albert Siegbahn	Lecturer	Department of Physics, Stockholm University, Sweden
Brock Sishc	Ph. D. student	Colorado State University

The course was publicized by e-mail notifications using the contact lists for the previous course and the 2012 Microbeam Workshop and by announcements on the RARAF and the EURADOS web sites.

Applicants and Students

- We received 25 applications. The prospective students were from the U.S, Europe and Asia and, as in the previous courses, covered a wide range of educational levels.
- The eight applicants selected for the course are listed in Table III and shown in Figure 5.
- David Welch, a new RARAF Postdoctoral Fellow, also participated in the training.
- As before, candidate selection was made by the RARAF Local Executive Committee, with scores applied based on a set of predetermined criteria.

Course

DAY 1:

- Followed essentially the same format as the first two courses, with the addition of a guest lecture by Dr. Eduoard Azzam from Rutgers University.
- As before, a live demonstration was given of the immediate production of a focus in cells with GFP-tagged XRCC1 protein using the charged particle microbeam.
- The day ended with a new session on the planning and experimental design of microbeam irradiations.

DAY 2:

- Followed the format of last year with demonstrations, hands-on activities (Figure 6), and intense debriefings.
- In addition, the students were tasked with designing an experiment based on their own scientific interest using knowledge obtained during the course to create a RARAF beam time request proposal.

DAY 3:

- Followed the format of the previous years, with lectures and group discussions and an in-depth tour of the x-ray, and neutron microbeams and the UV microspot.
- The lectures were followed by an intense discussion on user/facility interfacing.
- The students made presentations of their individual or team beam-time proposals for review and critique by the instructors.
- The course ended with an informal closing ceremony and the delivery of a certificate of completion to each student.

Each student took home a notebook containing copies of all the slides from the lectures as well as the instructions for all the physics and biology procedures that were demonstrated and that they had performed.

A virtual course created from the lectures and demonstrations from the past two years is described under "Dissemination" below. A paper on the design of and our experience with the training course has been published.

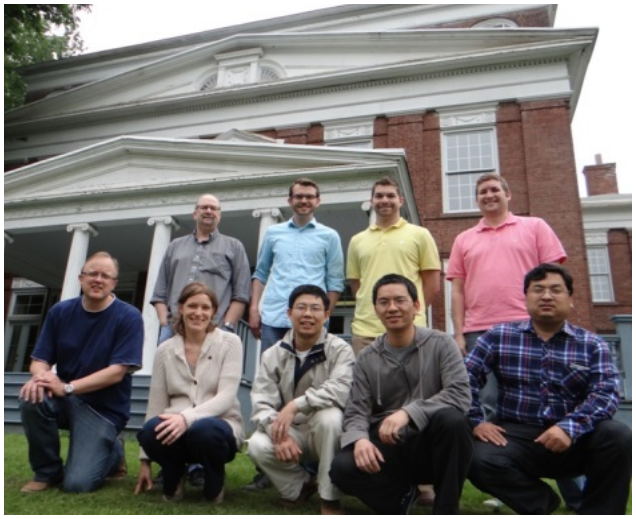

Figure 5. *The students for the third RARAF Microbeam Training Course outside the Nevis Mansion House.*

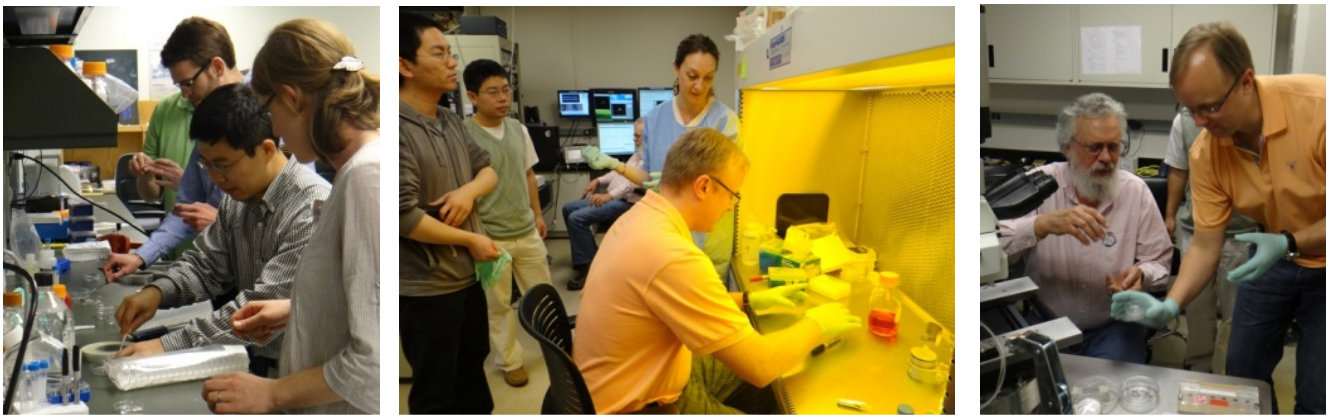

Figure 6. *Microbeam Training Course students engaging in hands-on training.*

Group Training

In addition to training individuals at RARAF, staff members also participate in training courses presented at other facilities as a means of introducing microbeam concepts and experiments to a broader audience. As for the past two years, Gerhard Randers-Pehrson lectured on "High/low LET microbeams" at the NASA Space Radiation Summer School, Brookhaven National Laboratory, Upton, NY, on June 14, 2013.

Dissemination

Web site

A new RARAF website design was created last year that provides clear and effective presentation and improves access to content. The RARAF website features a more modern look. Functional menus (including a home page rotating-picture menu) were designed to make navigation through the content easy and interesting, with a hierarchical structure from general information, suitable for a general or non-science audience, to more-detailed technical content.

The site contains information on microbeams in general, as well as detailed technical information on our various microbeams; *in-vitro* and *in-vivo* endpoints that we use; details of available on-line and off-line imaging capabilities; microfluidic systems we are developing; other charged particle and neutron irradiation facilities available at RARAF; our on-line training course materials; publications lists; information on RARAF contacts and directions to the facility. The site is periodically updated to include new radiation facilities, cell handling and analysis capabilities, publications and other information.

Virtual training course

Last year we developed an on-line virtual microbeam training course, based on the three-day microbeam training courses. This on-line course was designed to give interested physicists and biologists who could not attend in person a thorough introduction to microbeam technology.

The goal of the online course, as for the face-to-face course, is to facilitate a better understanding of how microbeams work, what experiments can be performed using a microbeam, why these experiments are of biological interest, and how to design / perform these experiments.

The on-line material curriculum consists of audio podcasts and the same handouts that the face-to-face students received. The audio of each podcast is synched with the accompanying PowerPoint slides (viewable on a video iPod, tablet, PC or Mac, or smart phone), as well as a PDF version of the slides. High-resolution video (720p, with audio) was also used to document demonstrations of all aspects of a microbeam experiment, from making microbeam dishes to irradiating cells and performing online analyses. After extensive editing, this resulted in about 4½ hours of video footage. Additional material is added to the on-line course for new course presentations or lecturers.

The on-line training course can be accessed through the RARAF website (www.RARAF.com), or through the RARAF YouTube channel (http://www.youtube.com/user/RARAFcourses). The videos can be viewed on any Internet-enabled device supporting YouTube format.

Tours

In addition to training students, tours of the Facility provide a general introduction to the research performed at RARAF and the irradiation facilities that are available. This year we gave tours to more than 30 scientists, students, and members of the public.

As an example, eleven high school seniors who had been offered priority admission to Columbia as physics majors, some of whom were Columbia I. I. Rabi Scholarship winners, toured RARAF in April along with Dr. John Parsons from the Physics Department at Nevis Labs.

Personnel

The Director of RARAF is Dr. David Brenner, the Director of the Center for Radiological Research (CRR).

The accelerator facility is operated by Mr. Stephen Marino, the Manager, and Dr. Gerhard Randers-Pehrson, the Associate Director of RARAF.

Dr. Charles Geard, a Senior Biologist Emeritus, continues to visit RARAF frequently lending his considerable expertise.

Dr. Brian Ponnaiya, an Associate Research Scientist, is the biology advisor for RARAF. He collaborates with many of the external users and coordinates with the CRR, where he spends about half his time.

Dr. Alan Bigelow, an Associate Research Scientist, developed the multiphoton microscopy system, which includes the UV microspot irradiation facility, and is working on the development of the Raman spectroscopy and AMOEBA systems.

Dr. Guy Garty, an Associate Professor, developed the Flow and Shoot (FAST) system and is developing the CE-LIF system. He spends about half his time working on the CRR National Institute of Allergy and Infectious Diseases (NIAID) project, for which he is the project manager.

Dr. Andrew Harken, an Associate Research Scientist, is responsible for the x-ray microbeam. He is also working on the imaging of cells without stain using a highly sensitive EMCCD camera, the STED system for extremely high-resolution spectroscopy, and the microFACS system.

Dr. Yanping Xu, an Associate Research Scientist, is developing the neutron microbeam. He is also developing the accelerator-generated Hiroshima atomic bomb spectrum neutron source.

Dr. Manuela Buonanno, a Postdoctoral Fellow in radiation biology, collaborates with many of external users and performs the assays for the mouse ear microbeam irradiations.

Dr. David Welch joined RARAF in May as a Postdoctoral Fellow after receiving a degree in biomedical engineering from Arizona State University. His expertise in microfluidics has been of considerable assistance in the development of our microfluidics applications.

RECENT PUBLICATIONS OF WORK PERFORMED AT RARAF

1. Azzam, E.I., de Toledo, S.M., Harris, A.L., Ivanov, V., Zhou, H., Amundson, S.A., Lieberman, H.B. and Hei, T.K. The ionizing radiation-induced bystander effect: Evidence, mechanism, and significance. Pathobiology of Cancer Regimen-Related Toxicities, Sonis, S.T., and Keefe, D.M., eds., pp.35-61. Springer, New York, NY, 2013. (Book chapter).
2. Bigelow, A.W., Ponnaiya, B., Targoff, K. and Brenner. D.J. UV microspot irradiator at Columbia University. Radiat. Environ. Biophys. **52**: 411-417 (2013), PMCID: PMC3723145.
3. Buonanno, M., Garty, G., Grad, M., Gendrel, M., Hobert, O. and Brenner, D.J. Microbeam irradiation of *C. elegans* nematodes in microfluidic channels. Radiat. Environ. Biophys. **52**: 531-537 (2013), PMCID: PMC3809145.
4. Grabham, P., Sharma, P., Bigelow, A. and Geard, C. Two distinct types of the inhibition of vasculogenesis by different species of charged particles. Vascular Cell **5**: 16 (2013), PMCID: PMC3856512.
5. Grad, M. "The Integration of Active Silicon Components into Polymer Microfluidic Devices" (Columbia University Ph. D. Thesis), 2013.
6. Grad, M., Bigelow, A.W., Garty, G., Attinger, D. and Brenner D.J. Optofluidic cell manipulation for a biological microbeam. Rev. Sci. Instrum. **84**: 014301 (2013), PMCID: PMC3562345.
7. Grad, M, Young, E.F., Smilenov, L., Brenner, D.J. and Attinger, D. A simple add-on microfluidic appliance for accurately sorting small populations of cells with high fidelity. J. Micromech. Microeng. **23**: 117003 (2013), PMCID: PMC3883503.
8. Hu, B., Zhu, J., Zhou, H., and Hei, T.K. No significant level of inheritable interchromosomal aberrations in the progeny of bystander primary human fibroblast after alpha particle irradiation. Adv. Space Res. **51**: 450-457 (2013), PMCID: PMC 3596834.
9. Lyulko, O.V., Randers-Pehrson, G. and Brenner, D.J. Simultaneous immersion Mirau interferometry. Rev. Sci. Instrum. **84**: 053701 (2013), PMCID: PMC3656945.
10. Ponnaiya, B., Amundson, S.A., Ghandhi, S.A., Smilenov, L.B., Geard, C.R., Buonanno, M., and Brenner, D.J. Single-cell responses to ionizing radiation. Radiat. Environ. Biophys. **52**: 523-530 (2013), PMCID: PMC3812812.
11. Riquier, H. "Étude des effets de radiations par rayons X ou par particules alpha sur les interactions entre cellules tumorales et cellules éndotheliales" ("Study of the effects of X-ray or alpha particle irradiations on the interplay between tumor cells and endothelial cells") (University of Namur, Belgium Ph. D. Thesis), 2013.
12. Xu, Y., Turner, H.C., Garty, G. and Brenner, D. A rapid, quantitative method to characterize the human lymphocyte concentration for automated high-throughput radiation biodosimetry. Biomed. Eng. Res. **2**: 16-19 (2013), PMCID: PMC3683596.
13. Zhang, B, Davidson, M.M., Zhou, H., Wang, C., Walker, W.F. and Hei, T.K. Cytoplasmic irradiation results in mitochondrial dysfunction and DRP1-dependent mitochondrial fission. Cancer Res. **73**: 6700-6710 (2013), PMCID: PMC3934017.

14. Zhang, S., Wen, G., Huang, S.X., Wang, J., Tong, J. and Hei, T.K. Mitochondrial alteration in malignantly transformed human small airway epithelial cells induced by alpha particles. Int. J. Cancer. **132**: 19-28 (2013), PMCID: PMC3467313.

15. Zhu, J., Shang, J., Brenner, D. and Lin, Q. An elastomeric polymer microchip for mechanically tunable cell trapping. In Proceedings of the 2013 IEEE Int. Conference on Micro Electro Mechanical Systems (MEMS '13), Taipei, Taiwan, January 20-24, 2013, pp. 945-948.

16. Zhu, J. Shang, J., Jia, Y., Liu, K., Brenner, D. and Lin, Q. Physical modulation based cell manipulation in microfluidic devices. In Proceedings of the 2013 IEEE Int. Conference on Nano/Micro Engineered and Molecular Systems (NEMS'13), Suzhou, China, April 7-10, 2013, pp. 1226-1229. ■

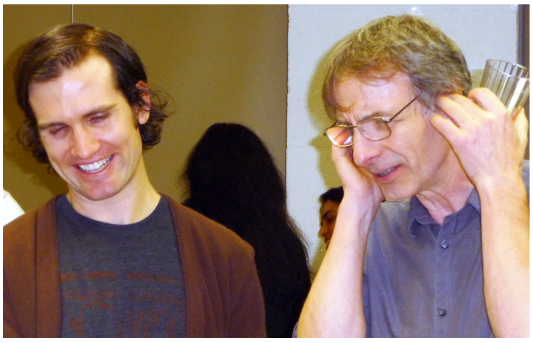

Top row (l to r): JD Knotts, Lubo Smilenov; Helen Turner, Igor Shuryak, Ana Vasileva, Gary Johnson, Suresh Kumar, David Welch, Mashkura Chowdhury, Jay Perrier, Rob Morton, Erica Pena, Margaret German. Second row (l to r): Ana Vasileva, Norm Kleiman. Third row (l to r): Radek Pieniazek, Dennis Keaveney; Cui-Xia Kuan; Gerhard Randers-Pehrson, Margaret German. Fourth row (l to r): Sunil Panigrahi, Sally Amundson, David Brenner, Howard Lieberman, Kevin Hopkins.